Effects of FeO/SiO$_2$ Ratio and Optical Basicity on Viscosity and Melt Structure of FeO–SiO$_2$–Al$_2$O$_3$–CaO–MgO–Cr$_2$O$_3$ Melts

J Isaksson[1], *A Andersson*[2], *A Lennartsson*[3], *F Gyakwaa*[4], *Q Shu*[5], *and C Samuelsson*[6]

1. Associate Senior Lecturer, Luleå University of Technology, Luleå Sweden 971 8. Email: Jenny.isaksson@ltu.se
2. Associate Senior Lecturer, Luleå University of Technology, Luleå Sweden 971 87. Email: anton.andersson@ltu.se
3. Senior Lecturer, Luleå University of Technology, Luleå Sweden 971 87. Email: andreas.lennartsson@ltu.se
4. Postdoc, University of Oulu, Oulu Finland FI-90014. Email: francis.gyakwaa@oulu.fi
5. Professor, University of Oulu, Oulu Finland FI-90014. Email: qifeng.shu@oulu.fi
6. Professor, Luleå University of Technology, Luleå Sweden 971 87. Email: caisa.samuelsson@ltu.se

Keywords: Iron silicate slag, viscosity, slag structure, copper slag

ABSTRACT

The physico-chemical property, viscosity, is essential for pyrometallurgical processes and influences the settling rate of valuable metal droplets in slag, affecting the metal recovery. The copper slag from smelting furnaces typically contains between 1 and 2 wt per cent Cu, which equals to or is higher than in most sulfidic copper ores mined today, meaning the slag is a valuable resource for copper extraction. A low viscosity is desirable for slag-cleaning through a settling furnace where entrained droplets settle under gravity. One approach to control the viscosity is through the slag composition. The literature has limited data on the correlation between viscosity, slag structure, and optical basicity of iron silicate slag with FeO/SiO_2, CaO, and Al_2O_3 as factors. Therefore, the present study evaluated the influence of these factors on viscosity and correlations with slag structure and optical basicity. The FeO/SiO_2 ratio (at per cent /at per cent) and the CaO and Al_2O_3 content were altered in two levels, resulting in a two-level full factorial design with three factors. The study was done by synthesising $FeO–SiO_2–Al_2O_3–CaO–MgO–Cr_2O_3$ melts, followed by water granulation. The melt structure of the samples was analysed with the help of Raman Spectroscopy. The viscosity was then estimated with a high-temperature rheometer using a Mo spindle and crucible. The results showed a correlation between the optical basicity, FeO/SiO_2 ratio, and viscosity, where a high optical basicity and FeO/SiO_2 ratio were beneficial for achieving a low melt viscosity.

INTRODUCTION

The slag viscosity in pyrometallurgical processes is crucial for determining the efficiency of metal extraction. It impacts various aspects of the extraction process, including tapping and handling of the slag (Bellemans et al, 2018) to mass and heat transfer (Kucharski et al 1989), refractory life, freeze lining on a water-cooled reactor (Bellemans, Zietsman and Verbeken, 2022; Nagraj, 2022), the kinetics of slag-metal reactions (Viswanathan, Sichen and Seetharaman, 2001), and the settling rate of metal-containing droplets in slag (Isaksson et al 2023b; Stokes, 1850). The increasing global demand for copper highlights the significance of raw material efficiency. Copper losses to slag represent a limiting factor, making it crucial to understand and control slag viscosity for optimising pyrometallurgical extraction of metals.

In the context of pyrometallurgical copper extraction, copper is distributed as entrained droplets and dissolved copper in the slag matrix. The entrained droplets can be recovered through slag cleaning operations, including a settling furnace where droplets settle under gravity. Slag from copper smelting furnaces usually contains the oxides FeO and SiO_2, along with smaller amounts of Al_2O_3, CaO, MgO, and minor elements such as Cu, As, Sb, Sn, and Pb. Al_2O_3, CaO, and MgO are introduced to the process through the concentrate feeds, flux materials, other additives, or through the dissolution of the refractory material. Additionally, Al_2O_3 is introduced to the processes via recycling of, e.g., waste electrical and electronic equipment (Mostaghel et al, 2013). The presence of these components affects the phase equilibria and the distribution of components between the gas, slag, matte, and solid oxide phases. This is particularly important in a slag cleaning process, including settling, as the copper distributed as dissolved copper in the slag matrix limits the recovery.

Sineva et al (2020) showed through an equilibrium study that Al_2O_3, CaO, and MgO reduced the copper concentrations in the slag in a Cu-Fe-O-S-Si-Al-Ca-Mg system. This means that modifications of the slag can decrease the dissolved copper content, which enhances the recovery as part of the dissolved copper becomes entrained. Isaksson et al (2023b) showed that the industrial CaO modification of slag increased the copper recovery in a settling process. The improvement was attributed to decreased viscosity, increased copper droplet sizes, and decreased copper solubility. The viscosity influences the settling rate of entrained copper in slag, where a lower viscosity benefits a high settling rate. The impact of FeO/SiO_2, Al_2O_3, and CaO on viscosity in copper smelting slag is thus of interest for pyrometallurgical processes associated with copper extraction. Reduced copper losses enhance raw material efficiency, leading to a more sustainable extraction.

Moreover, the slag viscosity depends on the temperature, atmosphere, composition, and melt structure. The structure of silicate-based melts is affected by (i) the degree of polymerisation of the silicate network, (ii) the fitting of certain cations, e.g., $Al^{3+,}$ and (iii) the nature of network-breaking cations, e.g., Ca^{2+} and Mg^{2+} (Mills, 1993). In addition, the melt structure can be described with a basicity index, taking the relevant oxides in a smelting slag from copper extraction into account, namely the optical basicity. The optical basicity is calculated with Eq. 1 and 2.

$$\Lambda = \sum_{i=1}^{n} \Lambda_i N_i \qquad \text{(Eq. 1)}$$

$$N_i = \frac{x_i n_i}{\sum_{i=1}^{n} x_i n_i} \qquad \text{(Eq. 2)}$$

where Λ is the optical basicity of the melt, Λ_i is the optical basicity of the component i, N_i the equivalent fraction of oxide i in the melt, x_i the mole fraction of component i in the melt, and n_i is the number of oxygen atoms in oxide i. Duffy (1989) introduced the measure of optical basicity to metallurgical slags and showed that the optical basicity of various oxides could be calculated from Pauling electronegativities. Duffy and Ingram (1992) presented values of the optical basicity, and the relevant values for this paper are presented in Table 1.

TABLE 1 - Optical basicities of individual oxides (Duffy and Ingram, 1992).

Oxide	Optical basicity
CaO	1
FeO	1
MgO	0.78
Al_2O_3	0.60
SiO_2	0.48
Cr_2O_3	0.8

Building on this idea, the present study investigated the influence of optical basicity on the slag viscosity and structure of melts related to pyrometallurgical copper extraction. It involved measuring the high-temperature viscosity of the synthetic FeO-SiO_2-Al_2O_3-CaO-MgO-Cr_2O_3 melts and analysing the structure of granulated samples with varying FeO/SiO_2 ratios, Al_2O_3 content and CaO content. The study contributes insight into the correlation between optical basicity, viscosity and melt structure. The obtained information can be used industrially to obtain smooth pyrometallurgical operations focusing on slag handling and improving slag cleaning, including a settling process. A decreased copper content in the slag will increase the efficiency of raw materials.

EXPERIMENTAL

The influence of composition and optical basicity on viscosity and melt structure was estimated in a two-level full-factorial design of experiments with the factors Al_2O_3 and CaO content and the FeO/SiO_2 ratio. The targeted sample compositions, FeO/SiO_2 ratio and the calculated optical basicity are shown in Table 2. The valence state of iron was not analysed and assumed to be present as FeO. Chromium(III) oxide was included in the system as it is present in the slag related to the pyrometallurgical extraction of copper. Chromium comes into the process with, e.g., electronic scrap and refractories and is a nucleation agent in the slag, forming chromium-rich spinels (Isaksson et al 2021; Lennartsson et al 2015). Solid phases in a melt increase the viscosity (Wright et al 2020; Zhen, Zhang and Chou 2015), and thus, chromium was determined to be an essential component to include for a more accurate reflection of the industrial slag viscosity.

TABLE 2 – FeO/SiO_2 ratio, optical basicity and sample compositions.

Sample no	FeO/SiO_2 [at%/at%]	Optical basicity	FeO [at%]	SiO_2 [at%]	CaO [at%]	Al_2O_3 [at%]	MgO [at%]	Cr_2O_3 [at%]
1L	1.08	0.665	49.83	45.99	1.2	1.4	1.5	0.08
2L	1.08	0.660	47.95	44.27	1.2	5	1.5	0.08
3L	1.08	0.689	44.21	40.81	12	1.4	1.5	0.08
4L	1.08	0.684	42.34	39.08	12	5	1.5	0.08
1H	1.25	0.682	53.25	42.59	1.2	1.4	1.5	0.08
2H	1.25	0.676	51.23	40.99	1.2	5	1.5	0.08
3H	1.25	0.706	47.23	37.79	12	1.4	1.5	0.08
4H	1.25	0.699	45.23	36.19	12	5	1.5	0.08

Sample Preparation

The slag samples of the experimental matrix were synthesised using the reagent-grade chemicals Fe, Fe_2O_3, SiO_2, $CaCO_3$, MgO, and Cr_2O_3. The dry chemicals were mixed, packed in Fe crucibles (>99.82 per cent Fe), and melted in a Ruhstrat resistance furnace in an inert atmosphere using N_2 (99.996 per cent) and Ar (99.999 per cent) with a flow rate of 12 L/h and 3 L/h respectively. Fe was used as a crucible material during the synthesis to provide an oxygen buffer to the system that would approach Fe-FeO conditions (Mysen and Richet, 2019). The Fe crucible thus ensures that a partial pressure of oxygen relevant to iron silicate slags undergoing a zinc-fuming process is attained during the synthesis (Andersson et al, 2023a).

The material was heated at 10 K/min until the temperature reached 100 K above the calculated liquidus temperature using the Equilib module of FactSage 8.2 (Bale et al, 2016) and the database GTOx. The melt was held at the temperature for one hour, removed manually from the furnace, and granulated in water jets with cold tap water at a flow rate of 1.1 L/s. Andersson et al (2023b) have published additional information about the granulation procedure.

Rheological Measurements

The rheological measurements were performed using the rotating cylinder technique and a Mo spindle and crucible (tzm molybdenum 364). The rheometer system was an Anton Paar Furnace Rheometer System (FRS 1800) (Anton Paar GMbH, 2022). More details about the rheometer can be found in a previous study (Isaksson et al 2023a). The temperature registered during the viscosity measurements was measured with a B-type thermocouple positioned in a hollow Al_2O_3 shaft holding the crucible, approximately 5 mm from the bottom of the melt. Ar (99.999 per cent) was introduced into the furnace via the crucible shaft, using a constant flow rate of 2.5 L/min. Figure 1 illustrates the rheometer employed in the experiments.

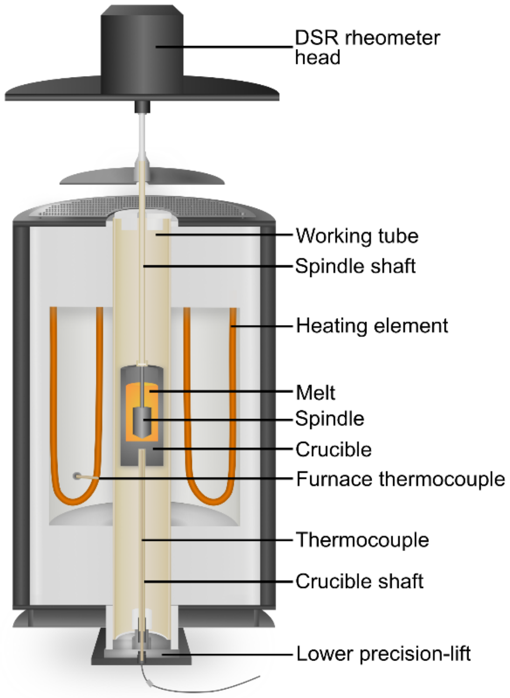

FIG 1 – Schematic overview of the rheometer setup.

The spindle was lowered when the heating started and descended continuously as the material melted until it reached the measuring position, 9 mm above the crucible bottom. The viscosity was measured during the cooling cycle every 50 K starting at 1723 K. Before viscosity measurement at a specific temperature started, the furnace was held at the target temperature for at least 45 min while rotating the spindle (shear rate of 4 1/s). This was done to reach a homogeneous temperature in the melt. A constant viscosity at a fixed shear rate indicated that the melt had homogenised. An automated program measured the viscosity with different constant shear rates of 1, 2, 4, 8, and 16

1/s. When the measurements were finalised, the samples were cooled with the natural cooling of the furnace while maintaining the Ar atmosphere.

Raman Spectroscopy

A representative sample of the granulated materials was ground using a ring mill. X-ray diffraction (XRD) was used to estimate if the samples were amorphous. The scans were performed with a Malvern Panalytical Empyrean X-ray diffractometer (Malvern Panalytical, Malvern, UK) operating on copper K_α generated at 45 kV and 40 mA. The scans were performed between 10 and 90 °2θ. The refinement was performed using HighScore+ and the FIZ Karlsruhe inorganic crystal structure database.

The ground samples were also analysed using Raman spectroscopy to determine the melt structure and the influence of FeO/SiO_2 ratio, Al_2O_3 and CaO. The Raman spectra of samples were collected in the 100–2000 cm^{-1} spectral range by a confocal micro-Raman spectrometer from B&W Tek (Plainsboro, US) with an excitation wavelength of 532 nm. Spectra were deconvolved by fitting the peaks corresponding to vibrations of various structural units using Gaussian line shapes (Mysen et al, 1982). The full widths of half maximum (FWHM) of various peaks were fixed to reduce the uncertainty of deconvolution.

RESULTS AND DISCUSSION

Viscosity Measurements

The viscosity measured at 1723 K and 1673 K are presented in Table 3 and plotted against the optical basicity in Figure 2. Overall, the viscosity for each composition increased with decreasing temperature. An increased temperature means increased kinetic energy in the melt, which increases the random motions of atoms and molecules, facilitating the migration of particles, and decreasing the internal friction in the fluid and, thus, the viscosity.

TABLE 3. Viscosity data obtained at 1723 K and 1673 K.

Sample no	**Viscosity [Pa·S]**	
	1723 K	**1673 K**
1L	0.132	0.16
2L	0.160	0.204
3L	0.074	0.091
4L	0.089	0.111
1H	0.089	0.111
2H	0.108	0.134
3H	0.055	0.067
4H	0.073	0.089

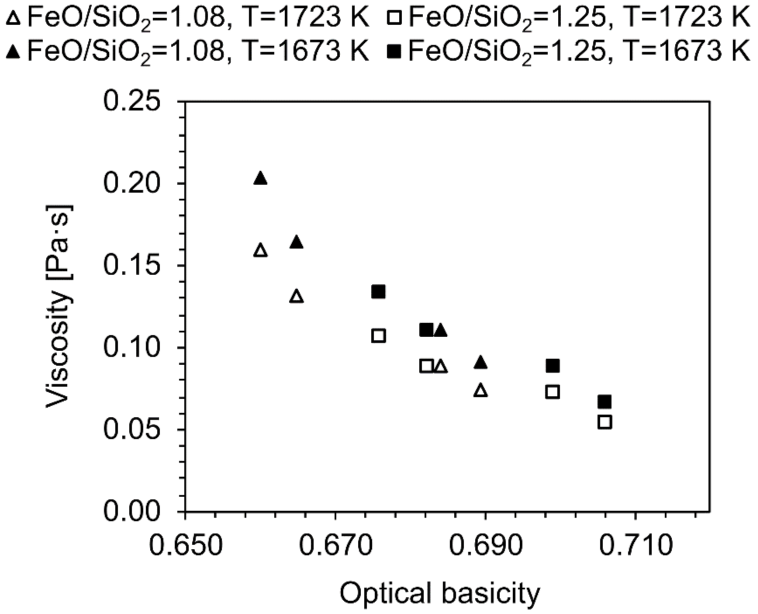

Fig 2 – Viscosity at 1723 K and 1673 K plotted against optical basicity.

The melt contains mainly iron and silica, where silica forms a silicate network. Molten silicate oxide systems consist of three-dimensional networks of SiO_4^{4-} tetrahedra where there are three types of oxygen: (1) bridging, (2) non-bridging, and (3) free oxygen (Mysen, 2003). The covalent bond between the silicon and oxygen atoms in the silicate network is resistant to motion, meaning a high silicate content has higher internal friction and, thus, higher viscosity. Adding basic oxides to the melt decreases the viscosity as the cat ion breaks the covalent bond between the silicon and oxygen atom, resulting in non-bridging oxygen or free oxygen in the structure and a more depolymerised slag. Optical basicity is an index of the amount of basic and acidic components within a system. The results showed that the viscosity decreased when increasing the optical basicity of the melt. At lower temperatures (1623–1423 K), the effect of optical basicity on viscosity remained but became more pronounced.

Evaluating the effect of the factors individually, it was concluded that CaO had the most significant effect on the viscosity, followed by the FeO/SiO_2 ratio. The effect of CaO addition on the viscosity has been examined with similar results, where the viscosity decreased with the CaO addition (Ducret and Rankin, 2002; Kaiura, Toguri and Marchant, 1977; Selivanov et al 2015; Shen et al 2019; Yan et al 2019; Zhang et al 2019), which supports the effect of CaO on viscosity in this study.

The melt with a high FeO/SiO_2 ratio and a high CaO and Al_2O_3 content has the second-highest optical basicity. However, it can be seen that the viscosity is deviating from the trend, with a higher viscosity than expected. The explanation is that Al_2O_3 can act as a network-forming oxide in the melt structure, meaning the increased Al_2O_3 content increases the melt viscosity. When Al_2O_3 acts as a network-forming oxide, it connects to free oxygen in the melt, forming the tetrahedra (AlO_4^{-5}). These findings align with the study by Mostagel et al (2013), which investigated the impact of Al_2O_3 additions on viscosity in an industrial iron silicate slag. Their results showed an increase in viscosity corresponding to higher Al_2O_3 content. Park et al (2011) demonstrated the amphoteric behaviour of Al_2O_3 while examining the influence of Fe/SiO_2 ratio and Al_2O_3 content on viscosity in a FeO_t-Al_2O_3-SiO_2 system. The results indicated an initial increase in viscosity with the addition of Al_2O_3, reaching a minimum before rising at higher Al_2O_3 concentrations. This behaviour was attributed to the amphoteric behaviour of Al_2O_3, wherein it initially acts as a basic oxide and shifts to an acidic oxide with the changes in slag composition (Park, Park and Sohn, 2011).

The lowest viscosity was obtained when the FeO/SiO_2 ratio and CaO content were high and the Al_2O_3 content was low. From an industrial perspective aiming for a slag with low viscosity, it is beneficial to operate with lower SiO_2 additions to obtain a higher FeO/SiO_2 ratio and to modify the slag with CaO, contributing to a higher optical basicity of the slag.

Raman Spectroscopy

The XRD analysis confirmed that the slags were predominantly amorphous. However, in samples 1L and 2H, a peak corresponding to cristobalite was detected, and a peak corresponding to spinel was detected in samples 3H and 4H. The Raman spectra were analysed to characterise the water-granulated slag structure. The collected Raman spectra had envelopes in the medium frequency range (400–800 1/cm) and high frequency (800–1200 1/cm). The Raman bands within medium frequency correspond to the bending vibration of the oxygen bridge Si(Fe)-O-Si(Fe). The high-frequency envelopes were deconvoluted into individual bands by assuming a Gaussian line shape. This study adopts Q^n to represent the structural unit of the symmetric stretching band of (SiO_4^{4-}) tetrahedra, where n represents the number of bridging oxygen in the tetrahedra. Q^n is generally available in the silicate structure as monomer silicate units (Q^0), dimer silicate units (Q^1), chain-like silicate structures (Q^2) and sheet-like silicate structures (Q^3).

The high-frequency envelope can be deconvolved by the bands from stretching vibrations of Q^0 with a Raman shift of 810–830 1/cm (Baert et al 2011; Mysen, Seifert and Virgo, 1980a; Mysen et al, 1982; Nayak and Desa, 2018), Q^1 with a Raman shift 880–910 1/cm, Q^2 with a Raman Shift 970–990 1/cm and Q^3 with a Raman shift 1030–1060 1/cm (Baert et al 2011; Kashio et al, 1980; Li, Shu and Chou, 2014; Mysen, Seifert and Virgo, 1980a; Mysen, Virgo and Scarfe, 1980b; Mysen et al, 1982; Nayak and Desa, 2018; Park, 2012; Wang, Shu and Chou, 2011).

An example of the deconvolution results (sample 1L) is shown in Figure 3. The areas of individual peaks were calculated, and the relative percentages of Q^0, Q^1, Q^2 and Q^3 in various samples were calculated from areas of corresponding peaks and shown in Table 4. It can be seen that Q^0 and Q^1 are the most abundant structural units in the samples, which means that the silicate network in the melt structure of the samples was largely depolymerised.

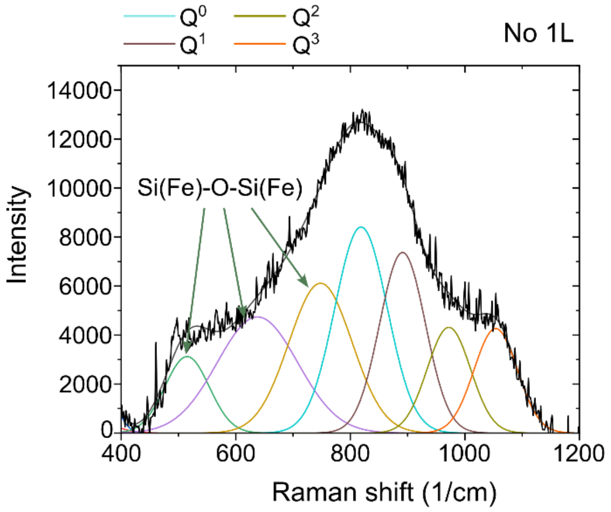

FIG 3 – The deconvolution results of sample 1L.

TABLE 4 – Relative per centages of Q^0, Q^1, Q^2, Q^3

Sample no	**Relative per centages**				**Q^0/Q^1**
	Q^0	**Q^1**	**Q^2**	**Q^3**	
1L	0.42	0.29	0.13	0.16	1.44
2L	0.42	0.28	0.14	0.16	1.48
3L	0.46	0.23	0.12	0.18	1.97
4L	0.49	0.23	0.08	0.19	2.11
1H	0.43	0.27	0.13	0.17	1.61
2H	0.43	0.26	0.15	0.16	1.64
3H	0.51	0.24	0.09	0.16	2.08
4H	0.50	0.23	0.10	0.18	2.19

Q^0/Q^1 ratios for various samples illustrate the variation of depolymerisation in the structure of slags with composition and are also listed in Table 4. The effects of FeO/SiO_2 ratios and additions of Al_2O_3 and CaO on structures of slags were investigated through calculated Q^0/Q^1 ratios. The samples with the same number but different letters can be compared to determine the effect of the FeO/SiO_2 ratio on the Q^0/Q^1 ratios, showing that a higher FeO/SiO_2 ratio leads to higher Q^0/Q^1 ratios, and thus a more depolymerised slag. For example, the Q^0/Q^1 ratios increased from 1.44 in 1L (low FeO/SiO_2 ratio) to 1.61 in 1H (high FeO/SiO_2 ratio), indicating that the 1H was more depolymerised. The effect of the FeO/SiO_2 ratio on the depolymerisation of the melt was in accordance with the study by Wang et al (2022).

The same data can be correlated to the viscosity measurements, where the samples with a higher FeO/SiO_2 had a significantly lower viscosity. These correlations confirm that a higher FeO/SiO_2 ratio leads to more depolymerised slag, decreasing the viscosity of the melt. The bond between silicon and oxygen is covalent, which is relatively resistant to motions; breaking this bond means that the internal friction in the material decreases, leading to lower viscosity.

Samples 3 and 4 (both L and H) have higher CaO contents than samples 1 and 2 (L and H). As seen in Table 4, the Q^0/Q^1 ratios for samples with a high CaO content are significantly higher than those with low CaO content. For example, 1L and 3L have the same composition besides the CaO content, which is higher in 3L. The Q^0/Q^1 ratio increases from 1.44 in 1L to 1.97 in 3L, indicating that the slag was more depolymerised in 3L. This indicates that CaO behaves as a network modifying oxide to depolymerise network structure. The depolymerisation effect on the viscosity was also confirmed, where the sample with higher CaO content had a lower viscosity.

For Al_2O_3, the content is higher in the even samples (2 and 4); when comparing the Q^0/Q^1 ratios, it indicates that Al_2O_3 (up to 5 at per cent) has a minor effect on the structure of the slag. However, the Q^0/Q^1 ratios were consistently higher when the Al_2O_3 content was higher, indicating that the melt structure became depolymerised when the Al_2O_3 content increased. The opposite trend was observed when comparing this data with the viscosity measurements. The viscosity was higher when the Al_2O_3 content was higher, indicating that Al_2O_3 acts as a network-forming oxide in the melt. One explanation for the decreased Q^0/Q^1 ratios may be because the increased content of Al_2O_3 reduces the absolute amount of SiO_2 in the samples, thus decreasing the relative amount of SiO_4^{4-} in the melt.

CONCLUSIONS

The present study investigated the correlation between optical basicity, viscosity, and the melt structure in a $FeO\text{-}SiO_2\text{-}Al_2O_3\text{-}CaO\text{-}MgO\text{-}Cr_2O_3$ system. The influence of the basicity was estimated in a two-level full-factorial design of experiments with the factors Al_2O_3 and CaO content and the FeO/SiO_2 ratio. Based on the experimental results, the following was concluded:

- The viscosity was lower in the melts with a higher optical basicity. A high FeO/SiO_2 ratio of 1.25 (at per cent /at per cent) and a high content of CaO was beneficial for obtaining a low viscosity. A higher content of Al_2O_3 (5 at per cent) increased the viscosity.
- The samples with a higher FeO/SiO_2 ratio resulted in a more depolymerised slag than those with a lower ratio (1.08 at per cent /at per cent). The samples with a higher CaO and Al_2O_3 content also resulted in a more depolymerised slag (higher Q^0/Q^1), according to the results from the Raman spectra. This indicates that the current analysis does not fully explain the melt structure when the Al_2O_3 content is higher.

The results from this study support the correlation between optical basicity, where samples with a higher optical basicity resulted in a more depolymerised slag with a lower viscosity. Indicating that optical basicity can be used as an index for the melt viscosity of $FeO\text{-}SiO_2\text{-}Al_2O_3\text{-}CaO\text{-}MgO\text{-}Cr_2O_3$ melts.

ACKNOWLEDGEMENTS

The present work was conducted in collaboration with Boliden through Bolidenpaketet and within the Center of Advanced Mining and Metallurgy (CAMM) at Luleå University of Technology, Sweden.

REFERENCES

Andersson, A, Brander, L, Lennartsson, A, Roos, Å, Engström, F, 2023a. A Method for Synthesizing Iron Silicate Slags to Evaluate Their Performance as Supplementary Cementitious Materials, *Applied Sciences*, 13.14:8357.

Andersson, A., Isaksson, J., Lennartsson, A., Engström, F., 2023b. Insights into the Valorization of Electric Arc Furnace Slags as Supplementary Cementitious Materials, *Journal of Sustainable Metallurgy*, 1–14.

Anton Paar GmbH, F., 2022. https://www.anton-paar.com/corp-en/products/details/furnace-rheometer-systems-frs-1600-and-frs-1800/. [Accessed 3.11.22].

Baert, K, Meulebroeck, W, Wouters, H, Cosyns, P, Nys, K, Thienpont, H, Terryn, H, 2011. Using Raman spectroscopy as a tool for the detection of iron in glass, *Journal of Raman Spectroscopy*, 42:1789–1795.

Bale, C W, Bélisle, E, Chartrand, P, Decterov, S A, Eriksson, G, Gheribi, A E, Hack, K, Jung, I H, Kang, Y B, Melançon, J, Pelton, A D, Petersen, S, Robelin, C, Sangster, J, Spencer, P, Van Ende, A D, 2016. FactSage Thermochemical Software and Databases, 2010-2016, *Calphad*, 54:35–53.

Bellemans, I, Cnockaert, V, De Wilde, E, Moelans, N, Verbeken, K, 2018. Metal Droplet Entrainment by Solid Particles in Slags: An Experimental Approach, *Journal of Sustainable Metallurgy*, 4:15–32.

Bellemans, I, Zietsman, J, Verbeken, K, 2022. Fundamental and Formation Aspects of Slag Freeze Linings: A Review, *Journal of Sustainable Metallurgy*, 8:64–90.

Ducret, A C, Rankin, W J, 2002. Liquidus temperatures and viscosities of $FeO-Fe_2O_3-SiO_2-CaO-MgO$ slags at compositions relevant to nickel matte smelting, *Scandinavian Journal of Metallurgy*, 31:59–67.

Duffy, J A, 1989. A common optical basicity scale for oxide and fluoride glasses, *Journal of Non-Crystalline Solids*, 109:35–39.

Duffy, J A, Ingram, M D, 1992. Comments on the application of optical basicity to glass, *Journal of Non-Crystalline Solids*,144:76–80.

Isaksson, J, Andersson, A, Lennartsson, A, Samuelsson, C, 2023a. Interactions of Crucible Materials With an FeO_x–SiO_2–Al_2O_3 Melt and Their Influence on Viscosity Measurements, *Metallurgical and Materials Transactions B*, 54:3526–3541.

Isaksson, J, Andersson, A, Vikström, T, Lennartsson, A, Samuelsson, C, 2023b. Improved Settling Mechanisms of an Industrial Copper Smelting Slag by CaO Modification, *Journal of Sustainable Metallurgy*, 9:1378–1389.

Isaksson, J, Vikström, T, Lennartsson, A, Samuelsson, C, 2021. Influence of Process Parameters on Copper Content in Reduced Iron Silicate Slag in a Settling Furnace, *Metals*, 11:1–15.

Kaiura, G H, Toguri, J M, Marchant, G, 1977. Viscosity of Fayalite-Based Slags. *Canadian Metallurgical Quarterly* 16:156–160.

Kashio, S, Iguchi, Y, Goto, T, Nishina, Y, Fuwa, T, 1979. *Raman Spectroscopic Study on the Structure of Silicate Slag, Transactions ISIJ*, 20:251–253.

Kucharski, M, Stubina, N M, Toguri, J M, 1989. Viscosity measurements of molten $Fe-O-SiO_2$, $Fe-O-CaO-SiO_2$, and $Fe-O-MgO-SiO_2$ slags, *Canadian Metallurgical Quarterly*, 28:7–11.

Lennartsson, A, Engström, F, Björkman, B, Samuelsson, C, 2015. Characterisation of buildup in an electric furnace for smelting copper concentrate, *Canadian Metallurgical Quarterly*, 54:477–484.

Li, J, Shu, Q, Chou, K, 2014. Structural Study of Glassy $CaO-SiO_2-CaF_2-TiO_2$ Slags by Raman Spectroscopy and MAS-NMR. *ISIJ International*, 54:721–727.

Mills, K C, 1993. The Influence of Structure on the Physico-chemical Properties of Slags. *ISIJ International*, 33:148–155.

Mostaghel, S, Matsushita, T, Samuelsson, C, Björkman, B, Seetharaman, S, 2013. Influence of alumina on physical properties of an industrial zinc-copper smelting slag: Part 1 - viscosity. *Mineral Processing and Extractive Metallurgy*, 122:42–48.

Mysen, B, 2003. Physics and chemistry of silicate glasses and melts, *European Journal of Mineralogy*, 15:781–802.

Mysen, B, Finger, L, Virgo, D, Seifert, F, 1982. Curve-fitting of Raman spectra of silicate glasses, *American Mineralogist*, 67:686–695.

Mysen, B, Richet, P, 2018. Silicate Glasses and Melts, 2nd ed. Elsevier.

Mysen, B, Seifert, F, Virgo, D, 1980a. Structure and redox equilibria of iron-bearing silicate melts, *American Mineralogist*, 65:867–884.

Mysen, B, Virgo, D, Scarfe C, 1980b. Relations between the anionic structure and viscosity of silicate melts- a Raman spectroscopic study, *American Mineralogist*, 65:690–710.

Nagraj, S, Chintinne, M, Guo, M, Blanpain, B, 2022. Investigation of Bath/Freeze Lining Interface Temperature Based on the Rheology of the Slag, *JOM*, 74:274–282.

Nayak, M T, Desa, J A E, 2018. Roles of iron and lithium in silicate glasses by Raman spectroscopy, *Journal of Raman Spectroscopy*, 49:1507–1513.

Park, H-S, Park, S S, Sohn, I, 2011. The Viscous Behavior of FeO_t-Al_2O_3-SiO_2 Copper Smelting Slags, *Metallurgical and Materials Transactions B*, 42:692–699.

Park, J H, 2012. Structure-property correlations of CaO-SiO_2-MnO slag derived from Raman spectroscopy, *ISIJ International*, 52:1627–1636.

Selivanov, E, Gulyaeva, R, Istomin, S, Belyaev, V, Tyushnyakov, S, Bykov, A, 2015. Viscosity and thermal properties of slag in the process of autogenous smelting of copper-zinc concentrates, *Mineral Processing and Extractive Metallurgy*, 124:88–95.

Shen, Y, Chong, J, Huang, Z, Tian, J, Zhang, W, Tang, X, Ding, W, Du, X, 2019. Viscosity and structure of a CaO-SiO_2-FeO-MgO system during a modified process from nickel slag by CaO, *Materials* 12:1–16.

Sineva, S, Fallah-Mehrjardi, A, Hidayat, T, Hayes, P C, Jak, E, 2020. Experimental Study of the Individual Effects of Al_2O_3, CaO and MgO on Gas/Slag/Matte/Spinel Equilibria in Cu-Fe-O-S-Si-Al-Ca-Mg System at 1473 K (1200 °C) and $p(SO_2) = 0.25$ atm, *Journal of Phase Equilibria and Diffusion*, 41:859–869.

Stokes, G G, 1850. On the Effects of the Internal Friction of Fluids on the Motion of Pendulums, *Transactions of the Cambridge Philosophical Society*, 9:75–129.

Viswanathan, N N, Ji, F Z, Sichen, D, Seetharaman, S, 2001. Viscosity measurements on some fayalite slags. *ISIJ International*, 41:722–727.

Wang, Z, Shu, Q, Chou, K, 2011. Structure of CaO-B_2O_3-SiO_2-TiO_2 Glasses: a Raman Spectral Study, *ISIJ International*, 51:1021–1027.

Wang, B, Yang, H, Jin, Z, Liu, Z, Zou, M, 2022. Effect of Fe/SiO_2 Ratio and Fe_2O_3 on the Viscosity and Slag Structure of Copper-Smelting Slags. *Metals*, 12:1–18.

Wright, S, Zhang, L, Sun, S, Jahanshahi, S, 2000. Viscosity of a CaO-MgO-Al_2O_3-SiO_2 Melt Containing Spinel Particles at 1646 K, *Metallurgical and Materials Transactions B*, 31: 97–104.

Yan, Z, Reddy, R G, Lv, X, Pang, Z, Bai, C, 2019. Viscosity of Iron Oxide Aluminosilicate Melts, *Metallurgical and Materials Transactions B*, 50:251–261.

Zhang, H, Fu, L, Qi, J, Xuan, W, 2019. Physicochemical Properties of the Molten Iron-Rich Slags Related to the Copper Recovery, *Metallurgical and Materials Transactions B*, 50:1852–1861.

Zhen, Y L, Zhang, G H, Chou, K C, 2015. Viscosity of CaO-MgO-Al_2O_3-SiO_2-TiO_2 Melts Containing TiC Particles, *Metallurgical and Materials Transactions B*, 46:155–161.